Research Article

The Application of the Vibration Absorber in Laser Inertial Navigation Products

Guoda Cheng,[1,2] **Yi Zhang** [2] **Hongjie Lei,**[2] **Pengyu Zhang,**[2] **Shengjun Wang,**[2] **and Xueying Li**[2]

[1]*Northwestern Polytechnical University, Xi'an 710072, China*
[2]*AVIC Xi'an Flight Automatic Control Research Institute, Xi'an 710076, China*

Correspondence should be addressed to Yi Zhang; 5zhangyi@tongji.edu.cn

The navigation accuracy of laser strap-down inertial navigation products declines with gyro dither, which is a bottleneck problem for the development of the important aviation instrument. The reason is that the dither of three gyros in the product couples and generates extra noise in the output signals of gyros. To decouple dither, this paper applies the vibration absorber in laser inertial navigation products. First of all, an angular vibration model of the three-rigid body system, which is constructed by the gyro, platform, and vibration absorber, is established. Then, the theoretical restriction of the absorber and the system response are derived. Finally, considering the power limitation for dither, the total power of the vibration system is analyzed. The analytical and experimental results show that the efficiency of the vibration absorber only relates to the frequency offset with gyros, and the absorber does lead to a sharp power increase.

1. Introduction

The dithered ring laser gyro (DRLG) is the most important sensor for inertial navigation products, the accuracy requirement of which is increasing in engineering. The characteristic where the output of DRLG keeps zero under small angular rate input is called the lock-in effect. To eliminate the lock-in effect, dither is involved in the operation of DRLG [1–3]. However, dithering coupled noise causes the accuracy of DRLG to sharply decrease in products [4]. The origin of dithering coupled noise is that the dither of one gyro excited the platform to dither, which changes the dynamic state of the other DRLG. As a result, the accuracy of other DRLG declines because of the platform dither [5, 6]. This paper attempts to apply the vibration absorber in inertial navigation products to eliminate dithering coupled noise. The theoretical contribution of this paper is to enhance the accuracy of DRLG in products via involving the absorber for angular vibration.

The previous study to decline the dithering coupled noise mainly focuses on the optimization of the damping system [7], the rational design of the inertial principal axis [8], the damper characteristic analysis [9], the lock-in error correction method [10, 11], and the increase of the moment of inertia of the platform [12–14]. The inertial measurement unit (IMU), which consists of accelerators, DRLG, and platform, of inertial navigation products is drawn in Figure 1.

The main idea of the above techniques is to make the vibration response of the platform as small as possible. The vibration absorber makes it possible for the platform to keep being motionless [6, 15]. The principle is to transfer the certain frequency vibration of the platform to the absorber. The absorber can be divided into the active form, passive form, half-active form, and hybrid form. The advantages of the passive absorber are simple structure, high reliability and stability, and no energy requirement. Therefore, the passive absorber has been widely used in aerospace, automotive, and other
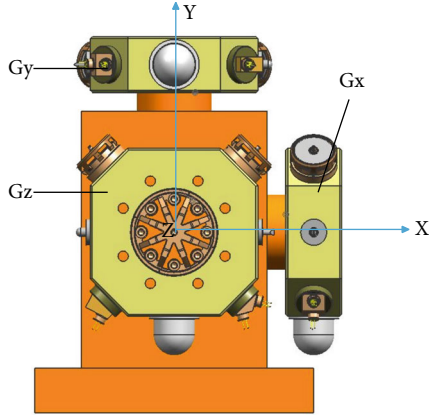
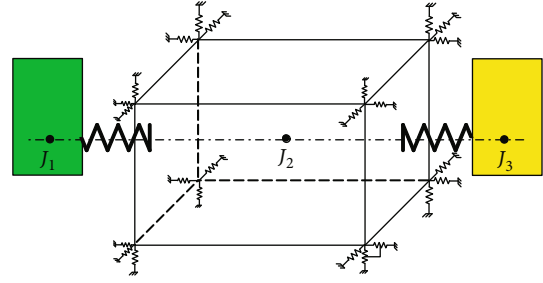FIGURE 1: The inertial measurement unit (the accelerators are hidden).

FIGURE 2: The three-rigid body angular vibration model of the DRLG-platform-absorber. The green rectangle stands for the DRLG, the transparent cuboid stands for the platform, and the yellow rectangle stands for the absorber.

fields. The innovation of this paper is to apply the absorber for angular vibration to DRLG, which dithers with a certain frequency.

This paper is organized as follows. The three-rigid body vibration model for the DRLG, platform, and absorber is established in Section 2, while the analytical expression of the total power of the system is derived in Section 3. Then, the simulations and experiments are illustrated in Section 4.

2. Vibration Modeling and Modal Analysis

Three DRLG in the IMU are dithering at the same time under the operational situation, as is shown in Figure 1. The axes of dithering are orthogonal. Therefore, it is reasonable to absorb the dithering of one DRLG first to simplify the derivation.

In general, the damping system of IMU consists of eight dampers under the symmetrical arrangement and the DRLG elastically connects with the platform. The three-rigid body system is illustrated in Figure 2. To avoid confusion, the moment of inertia mentioned below is calculated along the dotted line in Figure 2.

2.1. Vibration Modeling. The equation of motion for an undamped system is

$$\mathbf{M}\ddot{\mathbf{q}}(t) + \mathbf{K}\mathbf{q}(t) = \mathbf{Q}. \tag{1}$$

Specifically, for the angular vibration of the model along the dotted line in Figure 2, the moment of the inertia matrix is

$$\mathbf{M} = \begin{bmatrix} J_1 & 0 & 0 \\ 0 & J_2 & 0 \\ 0 & 0 & J_3 \end{bmatrix}, \tag{2}$$

where J_1 is the moment of inertia of the DRLG, J_2 is the moment of inertia of the platform, and J_3 is the moment of inertia of the absorber. The angular stiffness matrix is

$$\mathbf{K} = \begin{bmatrix} k_1 & -k_1 & 0 \\ -k_1 & k_1 + k_2 + k_3 & -k_3 \\ 0 & -k_3 & k_3 \end{bmatrix}, \tag{3}$$

where k_1 is the angular stiffness of the connection between the DRLG and the platform, k_2 is the angular stiffness of the connection between the ground and the platform, and k_3 is the angular stiffness of the connection between the absorber and the platform. The modal frequencies for the DRLG, the platform, and the absorber as a single DOF system are

$$\begin{aligned} \omega_1 &= \sqrt{\frac{k_1}{J_1}}, \\ \omega_2 &= \sqrt{\frac{k_2}{J_2}}, \\ \omega_3 &= \sqrt{\frac{k_3}{J_3}}. \end{aligned} \tag{4}$$

The response is

$$\mathbf{q} = [\theta_1 \theta_2 \theta_3]. \tag{5}$$

The generalized force is

$$\mathbf{Q} = \begin{bmatrix} M_1 & M_2 & M_3 \end{bmatrix}. \tag{6}$$

2.2. Modal Analysis. The eigenmatrix of this model [16] is

$$\mathbf{M}^{-1}\mathbf{K} = \begin{bmatrix} \dfrac{k_1}{J_1} & -\dfrac{k_1}{J_1} & 0 \\ -\dfrac{k_1}{J_2} & \dfrac{(k_1 + k_2 + k_3)}{J_2} & -\dfrac{k_3}{J_2} \\ 0 & -\dfrac{k_3}{J_3} & \dfrac{k_3}{J_3} \end{bmatrix}. \tag{7}$$

When the frequency of the absorber is equal to that of the DRLG, namely,

$$\omega = \frac{k_1}{J_1} = \frac{k_3}{J_3}, \tag{8}$$

the eigenmatrix can be written as

$$\mathbf{M}^{-1}\mathbf{K} = \begin{bmatrix} c_1 & -c_1 & 0 \\ -c_2 & c_3 & -c_4 \\ 0 & -c_1 & c_1 \end{bmatrix}. \tag{9}$$

For simplification, the expression of the eigenmatrix takes the following variable substitutions:

$$\begin{aligned} c_1 &= \frac{k_1}{J_1} = \frac{k_3}{J_3}, \\ c_2 &= \frac{k_1}{J_2}, \\ c_3 &= \frac{(k_1 + k_2 + k_3)}{J_2}, \\ c_4 &= \frac{k_3}{J_2}. \end{aligned} \tag{10}$$

One of the eigenvalues for the eigenmatrix is

$$\lambda = c_1. \tag{11}$$

The corresponding eigenvector is

$$\boldsymbol{\varphi} = \begin{bmatrix} -\dfrac{c_4}{c_2} & 0 & 1 \end{bmatrix} = \begin{bmatrix} -\dfrac{k_3}{k_1} & 0 & 1 \end{bmatrix} = \begin{bmatrix} -\dfrac{J_3}{J_1} & 0 & 1 \end{bmatrix}. \tag{12}$$

The eigenvector is the modal shape. And the corresponding modal frequency is

$$\omega = \sqrt{\lambda}. \tag{13}$$

Under the operational situation of IMU, the DRLG is dithering at the resonant frequency. Based on the theory of modal analysis, the mode according to ω will be excited and other modes will be suppressed. As a result, the response can be approximately written as

$$\mathbf{q} = A\begin{bmatrix} -J_3 & 0 & J_1 \end{bmatrix} \sin(\omega t), \tag{14}$$

where A is a constant related to the amplitude.

Equation (14) shows that when the absorber works, the resonance of the system occurs at the dithering frequency of DRLG. Since the platform keeps motionless, the design is not dependent on the limitation of its moment of inertia anymore. The amplitude of DRLG is inversely proportional to its moment of inertia, as well as the absorber.

3. Energy Analysis

Since the power to keep DRLG stably dithering is limited, the absorber cannot cost energy too much. The damper is the only dissipative cell. This section will analyze the total power of the system from the view of the damper.

3.1. Three-Rigid Body Model. According to the theory of modal analysis of the viscous damping assumption [16], the damping ratio of a single DOF system satisfies

$$\xi = \frac{d}{2\sqrt{mk}}, \tag{15}$$

where ξ is the damping ratio, d is the damping coefficient, m is the mass, and k is the stiffness.

The damping coefficients in Figure 2 can be calculated according to a single DOF system.

$$\begin{aligned} d_1 &= 2\xi_1\sqrt{J_1 k_1}, \\ d_2 &= 2\xi_2\sqrt{J_2 k_2}, \\ d_3 &= 2\xi_3\sqrt{J_3 k_3}. \end{aligned} \tag{16}$$

Then, the damping matrix of the three-rigid body model can be written as

$$\mathbf{C} = \begin{bmatrix} d_1 & -d_1 & 0 \\ -d_1 & d_1 + d_2 + d_3 & -d_3 \\ 0 & -d_3 & d_3 \end{bmatrix}. \tag{17}$$

The equation of motion with damper is

$$\mathbf{M}\ddot{\mathbf{q}}(t) + \mathbf{C}\dot{\mathbf{q}}(t) + \mathbf{K}\mathbf{q}(t) = \mathbf{Q}. \tag{18}$$

In steady-state vibration, potential energy and kinetic energy are reciprocally conversed to keep the conservation of system energy. The external input of energy is completely consumed by the damper. Regardless of the starting procedure, this paper focuses on the dissipation of dampers under the stably operating situation.

According to Equation (14) of the expression of the response, the damping torque is

$$\mathbf{Q}_c = \mathbf{C}\dot{\mathbf{q}} = \omega A \begin{bmatrix} d_1 & -d_1 & 0 \\ -d_1 & d_1 + d_2 + d_3 & -d_3 \\ 0 & -d_3 & d_3 \end{bmatrix} \begin{bmatrix} -J_3 \\ 0 \\ J_1 \end{bmatrix} \cos(\omega t). \tag{19}$$

Assuming the response of the system is $d\mathbf{q}$ in a very short time interval, the work of the damping torque in this interval is

$$dE = \mathbf{Q}_c{}^T d\mathbf{q} = \omega A^2 \begin{bmatrix} -J_3 \\ 0 \\ J_1 \end{bmatrix}^T \begin{bmatrix} d_1 & -d_1 & 0 \\ -d_1 & d_1+d_2+d_3 & -d_3 \\ 0 & -d_3 & d_3 \end{bmatrix}$$
$$\cdot \begin{bmatrix} -J_3 \\ 0 \\ J_1 \end{bmatrix} \cos(\omega t) d(\sin(\omega t)). \tag{20}$$

Specifically, the work in a quarter period can be integrated as

$$E_1 = \omega A^2 \int_{\omega t=0}^{\omega t=\pi/2} \begin{bmatrix} -J_3 \\ 0 \\ J_1 \end{bmatrix}^T \begin{bmatrix} d_1 & -d_1 & 0 \\ -d_1 & d_1+d_2+d_3 & -d_3 \\ 0 & -d_3 & d_3 \end{bmatrix}$$
$$\cdot \begin{bmatrix} -J_3 \\ 0 \\ J_1 \end{bmatrix} \cos(\omega t) d(\sin(\omega t)). \tag{21}$$

Taking $\tau = \omega t$, Equation (21) can be written as

$$E_1 = \omega A^2 \begin{bmatrix} -J_3 \\ 0 \\ J_1 \end{bmatrix}^T \begin{bmatrix} d_1 & -d_1 & 0 \\ -d_1 & d_1+d_2+d_3 & -d_3 \\ 0 & -d_3 & d_3 \end{bmatrix}$$
$$\cdot \begin{bmatrix} -J_3 \\ 0 \\ J_1 \end{bmatrix} \int_0^{\pi/2} \cos^2(\tau) d\tau. \tag{22}$$

Solving this integration, we can get

$$E_1 = \frac{\pi}{4} \omega A^2 \begin{bmatrix} -J_3 \\ 0 \\ J_1 \end{bmatrix}^T \begin{bmatrix} d_1 & -d_1 & 0 \\ -d_1 & d_1+d_2+d_3 & -d_3 \\ 0 & -d_3 & d_3 \end{bmatrix} \begin{bmatrix} -J_3 \\ 0 \\ J_1 \end{bmatrix}. \tag{23}$$

In addition, the total power can be calculated from the work in a quarter period.

$$p_1 = \frac{E_1}{T/4}. \tag{24}$$

The period and frequency keep the relationship below:

$$T = \frac{2\pi}{\omega}. \tag{25}$$

By substituting Equations (23) and ((25)) into Equation ((24)), we obtain the expression of power:

$$p_1 = \frac{1}{2}\omega^2(AJ_3)^2\left(d_1 + \left(\frac{J_1}{J_3}\right)^2 d_3\right). \tag{26}$$

3.2. Two-Rigid Body Model. Considering the power of single DRLG dithering for classical IMU, we simplify the system to the DRLG-platform two-rigid body model. As the stiffness of the damping system is far smaller than the stiffness between the DRLG and the platform, the working mode of the system can be regarded as a free mode. Therefore, the approximate response of the system is

$$\mathbf{q}_2 = B\begin{bmatrix} -J_2 & J_1 \end{bmatrix} \sin(\omega t). \tag{27}$$

Repeating the derivation in Section 3.1, we obtain the power of the two-rigid body model:

$$p_2 = \frac{1}{2}\omega^2(BJ_2)^2\left[d_1 + \left(\frac{J_1}{J_2}\right)^2 (d_1 + d_2)\right]. \tag{28}$$

Comparing the expressions of power for two models, we notice that when the amplitude of DRLG is a constant, i.e., $AJ_3 = BJ_2$, the power decreases with the increase of the moment of inertia of the absorber for the three-rigid body model, while the power decreases with the increase of the moment of inertia of the platform for the two-rigid body model.

4. Simulation and Experiment

Based on engineering experience, the damper, which is made of rubber, keeps a damping ratio of $\xi_2 = 0.1$, and the other connections are made of spring steels with a damping ratio of 0.005. In the simulations, the dithering frequency, moment of inertia, and dithering amplitude of the DRLG are assumed to be 500 Hz, $J_1 = 10^{-3}\text{kg} \cdot \text{m}^2$, and 1 arc-minute, respectively. The modal frequency of the damping system is assumed to be 50 Hz.

4.1. Simulation. First of all, the changing of modal frequencies and absorber response with the moment of inertia are illustrated in Figure 3.

It can be seen that with the increase of the moment of inertia of the absorber, the fundamental modal frequency and the second modal frequency remain constant, while the third modal frequency increases and the response of the absorber decreases. For the consideration of the control logic and reducing the structural deformation, it is better to enlarge the gap between the second modal frequency and the third frequency and depress the response of the absorber. Therefore, the moment of inertia of the absorber should be as large as possible. However, this does not coincide with the lightweight principle for the design of inertial navigation products. The eclectic principle is to enlarge the radius of gyration in the design of the absorber.

To ensure a single variable below, the moment of inertia of the absorber is assumed to be $J_3 = 10^{-3}\text{kg} \cdot \text{m}^2$.
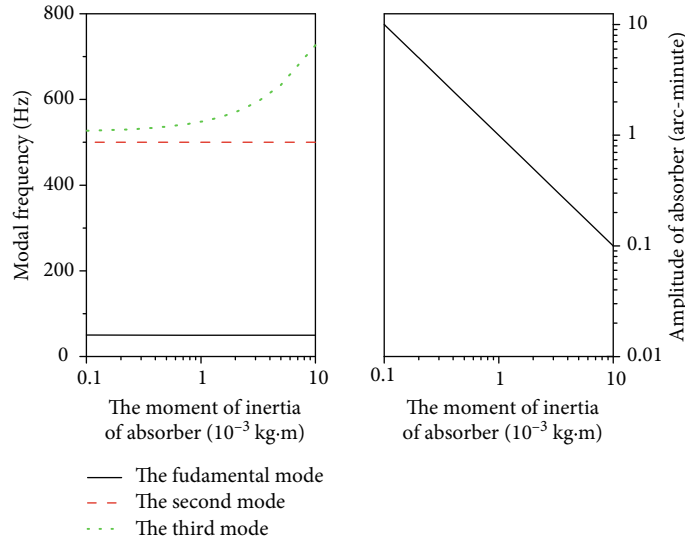
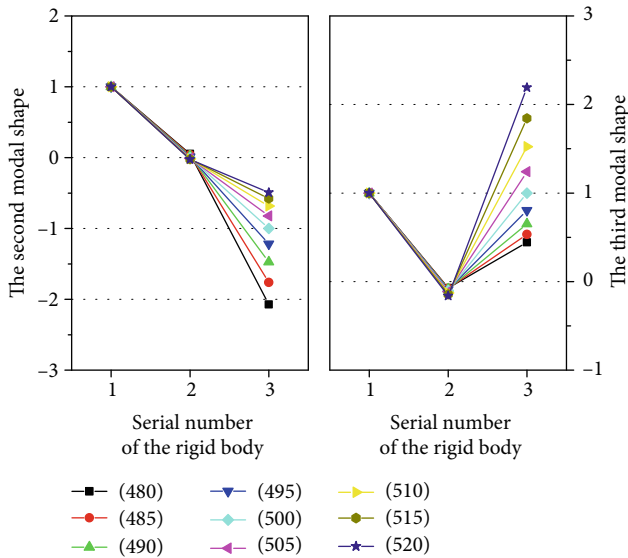Figure 3: The changing of the modal frequency and the amplitude of the absorber.

Figure 4: The modal shapes of higher modes.

Figure 5: The response of the platform under different frequencies of the absorber.

Secondly, it is valuable to discuss the performance of the absorber under the situation that its frequency is not exactly equal to the DRLG's frequency. When the modal frequency of the absorber is changed from 480 Hz to 520 Hz, the modal shapes of higher modes are illustrated in Figure 4.

It shows that for the second mode, the dithering of the DRLG and absorber is opposite in phase and the dithering of the platform is depressed. For the third mode, the dithering of the DRLG and absorber is identical in phase and the dithering of the platform is enlarged. To make the absorber work, it is important to change the control logic of the DRLG, which must dither at the second mode.

Finally, the total power of the mode with the absorber and the one without the absorber is calculated according to Section 3.

It is inevitable that the frequency of the absorber does not exactly match the frequency of the DRLG. To illustrate the
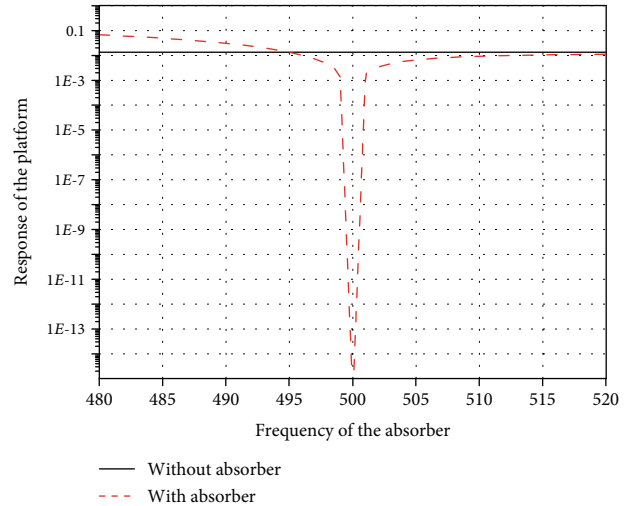
influence of mismatching of frequencies, the response of the platform under different frequencies of the absorber is drawn in Figure 5.

From Figure 4, we can see that the frequency bandwidth for the platform keeping lower vibration is about 1 Hz. Therefore, a frequency bias of 1 Hz between the absorber and the DRLG is set in power discussion. To verify the statement in Section 3.2 that the working mode of the two-rigid body system can be regarded as a free mode, the error of this assumption is shown in Table 1.

The table shows that the error of this assumption is about 1%. It is reasonable to employ moments of the platform and DRLG to derive the total power of the two-rigid body mode. When the moment of inertia of the platform is changed, the total power of both models is shown in Table 2.

It is shown that the total power of the two-rigid body mode dramatically decreases with the increase of the

TABLE 1: Comparison between the moment ratio and the response ratio of the platform to DRLG.

Moment ratio of the platform to DRLG	40	60	80	100	120
Response ratio of the platform to DRLG	39.6	59.4	79.2	99.0	118.8
Error(%)	1.1	1.1	1.0	1.0	1.0

TABLE 2: Comparison of the total power between two modes.

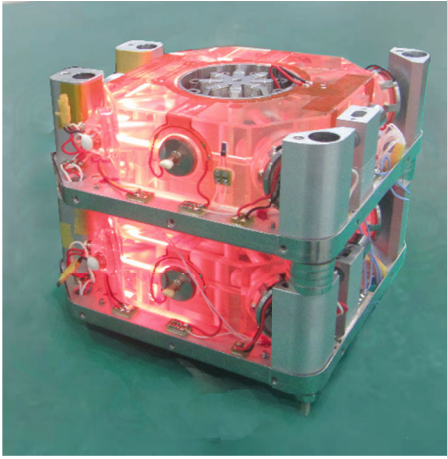| The moment of inertia of the platform (10^{-3}kg $\cdot$ m^2)	10	30	50	70	90	110
Two-rigid body mode (milliwatt)	40.7	22.3	18.6	17.1	16.2	15.6
Three-rigid body mode (milliwatt)	25.9	24.9	24	23.2	22.4	21.8

FIGURE 6: The absorber experiment.

moment of inertia of the platform. It matches with the fact that when the platform is light, the DRLG is not able to dither normally. The total power of the three-rigid body mode does not change a lot with the moment of inertia of the platform, and the extra power caused by the absorber is acceptable.

4.2. Experiment. To verify the feasibility of the absorber in inertial navigation products, an experiment is designed. In this experiment, two selfsame DRLG connect with a light platform, the upper one plays the role of the absorber via removing the dithering driver, and the under one is a normal DRLG, as is shown in Figure 6.

The control logic of the under DRLG is modified to avoid system resonance at the third mode. The result shows that the under DRLG works well without loss of accuracy, the platform keeps motionless, and even the upper DRLG, who is employed as the absorber, keeps normal accuracy.

5. Conclusion

The vibration absorber for the DRLG is discussed in this paper to solve the following problem: the dithering coupled noise pollutes the measured signal of DRLG. The accuracy of the DRLG in products can be improved with an absorber. It is promising that a well-designed DRLG with an absorber can be employed as the Zerolock Laser Gyro (ZLG) in products. A model of the DRLG, platform, and absorber is built

for modal analysis first. Then, energy analysis is presented for engineering practicability. Finally, the simulation and experiment contribute the conclusions below:

(1) The design of the absorber should follow the principle that the frequency of the absorber should be equal to that of the DRLG and the radius of gyration should be as long as possible

(2) The system must resonate at the second mode. Therefore, the control logic of the DRLG needs to be modified to avoid system resonance at the third mode

(3) The absorber energy cost is acceptable for the driver of the DRLG, and the DRLG can operate well with the absorber

Data Availability

The data used to support the findings of this study are available from the corresponding author upon request.

Conflicts of Interest

The authors declare that they have no conflicts of interest.

References

[1] W. W. Chow, J. Gea-Banacloche, L. M. Pedrotti, V. E. Sanders, W. Schleich, and M. O. Scully, "The ring laser gyro," *Reviews of Modern Physics*, vol. 57, no. 1, pp. 61–104, 1985.

[2] D. A. Andrews, S. Roden, and T. A. King, "A model for lock-in growth in ring laser gyroscopes," *IEEE Journal of Quantum Electronics*, vol. 31, no. 9, pp. 1709–1715, 1995.

[3] S. G. Roden, D. A. Andrews, C. Knipe, and T. A. King, "Proposed mechanism for lock-in growth in ring laser gyros," in *Proceedings of SPIE-The International Society for Optical Engineering*, pp. 208–219, Orlando, FL, USA, 1992.

[4] F. Fang, W. Zeng, and Z. Li, "Coupled dynamic analysis and decoupling optimization method of the laser gyro inertial measurement unit," *Sensors (Basel, Switzerland)*, vol. 20, no. 1, p. 111, 2020.

[5] Z. Liu, L. Wang, K. Li, J. Ban, and M. Wang, "A calibration method for the errors of ring laser gyro in rate-biased mode," *Sensors (Basel, Switzerland)*, vol. 19, no. 21, p. 4754, 2019.

[6] B. V. Klimkovich and A. M. Tolochko, "A correcting filter for a mechanically dithered single-axis ring laser gyro," *Gyroscopy and Navigation*, vol. 8, no. 1, pp. 43–50, 2017.

[7] Z. H. Tuo, D. W. Hu, R. H. Li, and J. C. Wei, "Damping design of strapdown inertial navigation system," *Journal of Chinese Inertial Technology*, vol. 17, no. 6, pp. 648–650, 2009.

[8] Z. H. Yao, H. J. Lei, H. W. Song, and Y. Zhang, "A refined modeling of the coupled vibration for laser strapline inertial navigation," *Journal of Vibration and Shock*, vol. 38, no. 21, pp. 271–277, 2019.

[9] Z. H. Tuo, J. X. Zhao, and M. P. Wu, "Simulation and optimization of heat-transfer route of isolator in a certain type of inertial navigation system," *Infrared and Laser Engineering*, vol. 36, no. z2, pp. 349–353, 2007.

[10] Z. Fan, H. Luo, G. Lu, and S. Hu, "Direct dither control without external feedback for ring laser gyro," *Optics & Laser Technology*, vol. 44, no. 4, pp. 767–770, 2012.

[11] Z. Fan, "Research on lock-in correction for mechanical dithered ring laser gyro," *Optical Engineering*, vol. 50, no. 3, article 034403, 2011.

[12] G. Li, G. Wei, Y. P. Xie, X. D. Yu, and X. W. Long, "Isotropic design method of suspension system of dithered RLG strapdown inertial measurement unit," in *International Conference on Frontiers of Energy*, Switzerland, 2014.

[13] J. Li, J. Fang, and S. Sam Ge, "Kinetics and design of a mechanically dithered ring laser gyroscope position and orientation system," *IEEE Transactions on Instrumentation & Measurement*, vol. 62, no. 1, pp. 210–220, 2013.

[14] J. Cheng, J. Fang, W. Wu, and J. Li, "Optimized design method of vibration isolation system in mechanically dithered RLG POS based on motion decoupling," *Measurement*, vol. 48, pp. 314–324, 2014.

[15] V. Piccirillo, "Suppression of chaos in nonlinear oscillators using a linear vibration absorber," *Meccanica*, vol. 56, no. 2, pp. 255–273, 2021.

[16] J. A. B. Faria, *Multiconductor Transmission-Line Structures: Modal Analysis Techniques*, Wiley, 1993.